



Estimating US fossil fuel CO₂ emissions from measurements of ¹⁴C in atmospheric CO₂

Sourish Basu^{a,b,1,2,3}, Scott J. Lehman^c, John B. Miller^a, Arlyn E. Andrews^a, Colm Sweeney^a, Kevin R. Gurney^d, Xiaomei Xu^e, John Southon^e, and Pieter P. Tans^a

^aGlobal Monitoring Laboratory, National Oceanographic and Atmospheric Administration, Boulder, CO 80305; ^bCooperative Institute for Research in Environmental Sciences, University of Colorado Boulder, Boulder, CO 80309; ^cInstitute of Arctic and Alpine Research, University of Colorado Boulder, Boulder CO 80309; ^dSchool of Informatics, Computing and Cyber Systems, Northern Arizona University, Flagstaff, AZ 86011; and ^eKeck Carbon Cycle AMS Facility, University of California, Irvine, CA 92697

Edited by Inez Fung, University of California, Berkeley, CA, and approved April 1, 2020 (received for review October 30, 2019)

We report national scale estimates of CO₂ emissions from fossil-fuel combustion and cement production in the United States based directly on atmospheric observations, using a dual-tracer inverse modeling framework and CO₂ and Δ¹⁴CO₂ measurements obtained primarily from the North American portion of the National Oceanic and Atmospheric Administration's Global Greenhouse Gas Reference Network. The derived US national total for 2010 is 1,653 ± 30 TgC yr⁻¹ with an uncertainty (1σ) that takes into account random errors associated with atmospheric transport, atmospheric measurements, and specified prior CO₂ and ¹⁴C fluxes. The atmosphere-derived estimate is significantly larger (> 3σ) than US national emissions for 2010 from three global inventories widely used for CO₂ accounting, even after adjustments for emissions that might be sensed by the atmospheric network, but which are not included in inventory totals. It is also larger (> 2σ) than a similarly adjusted total from the US Environmental Protection Agency (EPA), but overlaps EPA's reported upper 95% confidence limit. In contrast, the atmosphere-derived estimate is within 1σ of the adjusted 2010 annual total and nine of 12 adjusted monthly totals aggregated from the latest version of the high-resolution, US-specific "Vulcan" emission data product. Derived emissions appear to be robust to a range of assumed prior emissions and other parameters of the inversion framework. While we cannot rule out a possible bias from assumed prior Net Ecosystem Exchange over North America, we show that this can be overcome with additional Δ¹⁴CO₂ measurements. These results indicate the strong potential for quantification of US emissions and their multiyear trends from atmospheric observations.

fossil fuel CO₂ | radiocarbon | atmospheric inverse modeling

Anthropogenic emissions of CO₂ and other greenhouse gases (GHGs) are the leading cause of global mean temperature rise in the industrial era. This, along with increased documentation of the environmental, social, and economic consequences of associated sea-level rise and extreme weather events, has led the majority of nations to join in a declaration to limit man-made warming through Nationally Determined Contributions to global GHG emission-reduction targets as part of the 2015 Paris Climate Accord and its follow-up agreements. Although the United States has officially notified the United Nations that it will withdraw from the Accord, the obligation to report national annual emissions of CO₂ and other GHGs is independently mandated by the United Nations Framework Convention on Climate Change (UNFCCC), ratified by the United States in 1994. For the United States, this obligation is met by the Environmental Protection Agency (EPA), using accounting methods designed to provide year-to-year consistency and transparency of reporting (1). Although relative uncertainties for CO₂ emissions from fossil-fuel use and cement production (FF CO₂) are smaller than for other EPA-reported GHGs such as CH₄, FF CO₂ is by far the largest component of total CO₂-equivalent anthropogenic emissions and, therefore, dominates the overall

uncertainty in estimated total US contribution to climate forcing (ref. 2, table A-284). In the case of FF CO₂, estimates from the US EPA can be compared to FF CO₂ inventories commonly used for CO₂ accounting, such as from the Emissions Database for Global Atmospheric Research (EDGAR; ref. 3), the Carbon Dioxide Information and Analysis Center (CDIAC, ref. 4; maintained until September 2017 by the US Department of Energy), and the recently updated Vulcan high-resolution US FF CO₂ emission data product (5) version 3.0 (6). While the presence of multiple inventories allows for cross-validation, the accuracy of "bottom-up" inventories depends on the ability to track all emission processes and their intensities, which is an intrinsically difficult task with uncertainties that are not readily quantified. On the other hand, distributed atmospheric observations of Δ¹⁴CO₂ (proportional to the ¹⁴C:C ratio in CO₂) are sensitive to fossil CO₂ emissions from all possible sources and can provide independent emission estimates with quantifiable errors that arise primarily from atmospheric transport modeling (7, 8). The strong detection capability arises from the fact that

Significance

The vast majority of the world's nations have pledged to reduce emissions of CO₂ and other greenhouse gases and to track and report emissions using accounting methods based on economic statistics and emissions factors. Here, we present an independent method of emissions monitoring based directly on atmospheric observations and the strong fossil fuel CO₂ detection capability afforded by precise measurements of ¹⁴CO₂ in air samples obtained largely from NOAA's air sampling network. The national total we derive for 2010 is larger than from available inventories, including the US EPA, but is within error bounds of the updated Vulcan emission data product. These results suggest that reported emissions can now be subject to independent and objective evaluation using atmospheric ¹⁴CO₂ measurements.

Author contributions: S.J.L. and J.B.M. conceived the study and, with P.P.T., built and coordinated NOAA's Δ¹⁴CO₂ program; S.B. performed the computational work; S.B. and S.J.L. wrote the paper; A.E.A. and C.S. oversaw tower and aircraft sampling within the Global GHG Reference Network (GGGRN); J.S. performed many of the accelerator mass spectrometry (AMS) measurements; X.X. contributed Δ¹⁴CO₂ data from Barrow, AK; K.R.G. provided Vulcan 3.0 data; and S.B., S.J.L., and J.B.M. contributed to the interpretation of results.

The authors declare no competing interest.

This article is a PNAS Direct Submission.

Published under the PNAS license.

¹To whom correspondence may be addressed. Email: sourish@umd.edu.

²Present address: Global Modeling and Assimilation Office, National Aeronautics and Space Administration, Goddard Space Flight Center, Greenbelt, MD 20771.

³Present address: Earth System Science Interdisciplinary Center, University of Maryland, College Park, MD 20740.

This article contains supporting information online at <https://www.pnas.org/lookup/suppl/doi:10.1073/pnas.1919032117/-DCSupplemental>.

CO₂ derived from fossil sources is devoid of ¹⁴C due to complete radioactive decay, while the atmosphere and other CO₂ sources are relatively ¹⁴C-rich due to ongoing production in the upper atmosphere.

Here, we develop and report a national-scale estimate of FF CO₂ based directly on atmospheric observations of CO₂ and Δ¹⁴CO₂. Our approach uses a dual-tracer atmospheric inverse modeling framework (8), assimilating observations obtained primarily from the North American portion of the National Oceanic and Atmospheric Administration's (NOAA's) Global GHG Reference Network (GGGRN) for 2010, the first year with sufficient Δ¹⁴CO₂ observational coverage for this purpose. Our results suggest that US FF CO₂ emission inventories can now be subjected to independent and objective evaluation at the national monthly scale. In addition, we show that the dual-tracer approach can be used to reduce biases in Net Ecosystem Exchange (NEE) that may otherwise arise from incorrect specification of FF CO₂ in more traditional, CO₂-only inversion frameworks.

Background

Much of our understanding of the long-term growth of atmospheric CO₂ and its causes is based on a monitoring program at NOAA's Global Monitoring Laboratory, which has led the world's largest atmospheric sampling and measurement effort since the early 1980s. While a global array of precise CO₂ observations, whether from existing surface sampling networks or future satellite programs, can be used to constrain the total net CO₂ surface flux at global to regional scales (e.g., refs. 9–11), it is not possible to use atmospheric CO₂ observations alone to estimate national or regional FF CO₂ because observed atmospheric CO₂ gradients over land are typically dominated by large and variable carbon exchange with the terrestrial biosphere. However, precise measurements of Δ¹⁴CO₂ in a subset of the same samples that provide the primary surface-based CO₂ observations now allow for accurate and precise (approximately ±1 part per million in a single air sample) determination of the recently added FF CO₂ component of total CO₂ (12–15), which, in turn, can be traced back to sources using inverse methods.

Measurement of Δ¹⁴CO₂ within the NOAA network began in 2003 (16) and reached ~900 measurements per year for the North American portion of the GGGRN in 2010. Although substantially less than the number of measurements recommended for international emissions verification by the US National Academy of Sciences (17), Observing System Simulation Experiments (OSSEs) indicate that the measurement coverage available in 2010 is sufficient to estimate annual total US emissions with an accuracy of a few percent if atmospheric transport is perfectly known (8).

In this work, we use the dual-tracer variational inversion framework of Basu et al. (8) to estimate gridded FF CO₂ for 2010 and bounding months of 2009 (November and December) and 2011 (January and February). Weekly fluxes are estimated at a resolution of 3° × 2° globally and 1° × 1° over North America and then spatiotemporally aggregated for reporting here. The majority of assimilated atmospheric CO₂ and Δ¹⁴CO₂ measurements are from the United States (895 of 984 Δ¹⁴CO₂ measurements in 2010). A list of sites and laboratories contributing Δ¹⁴CO₂ measurements is given in *SI Appendix, Table S2*. Our reported FF CO₂ estimate is the mean of three inversions using three different gridded prior FF CO₂ estimates, namely, “Miller/CT” (previously implemented in NOAA's CarbonTracker), Open-Data Inventory for Anthropogenic CO₂ (ODIAC; ref. 18), and Fossil Fuel Data Assimilation System (FFDAS; ref. 19). Seasonality of emissions in the ODIAC and FFDAS priors was based on scaling of their annual totals by the temporal profile of CDIAC monthly totals for 2009 to 2011

(20), while the monthly variation of Miller/CT emissions was imposed by scaling to a fixed seasonality from Blasing et al. (21). In addition, we performed sensitivity tests using versions of the Miller/CT and FFDAS priors in which the seasonal variation of emissions was removed. An example of mean annual prior FF CO₂ for North America is shown in Fig. 1, along with US CO₂ and Δ¹⁴CO₂ sampling locations. Differences between the other two FF CO₂ priors and Miller/CT over North America are given in *SI Appendix, Fig. S3*.

The reported uncertainty of FF CO₂ estimates from the inversion system is a close approximation of the exact posterior FF CO₂ uncertainty and is derived from a 110-member ensemble of independent inversions, across which we randomly perturb 1) prior CO₂ and ¹⁴C fluxes according to their prescribed uncertainties; and 2) CO₂ and Δ¹⁴CO₂ observations according to their long-term measurement uncertainties and their so-called “representativeness errors,” a component of the random transport model error associated with the attempt to represent point measurements with a finite-resolution transport model (22). A description of additional sensitivity tests and additional information regarding the observations, the inversion framework, and the derivation of uncertainties are given in *Materials and Methods*. To enable meaningful comparison, both atmosphere-derived FF CO₂ and FF CO₂ from gridded inventory products were aggregated within the limits of the same 1° × 1° US country mask. In addition, US total emissions from Vulcan 3.0 were adjusted to account for nonfossil CO₂ emissions from the combustion of biofuels in the transportation sector by using monthly estimates from the Energy Information Administration (ref. 23, section 11). Where necessary, adjustments were also made to inventory totals in order to account for emissions from in-country international and domestic aviation that might be sensed by the atmospheric sampling network, but which were excluded from some inventories. For international aviation, we summed estimates of emissions for 2010 occurring along international aviation tracks (all altitudes) within the limits of our US country mask (18). Estimates of emissions from domestic aviation in 2010 were taken from the US EPA (ref. 2, table 2-13).

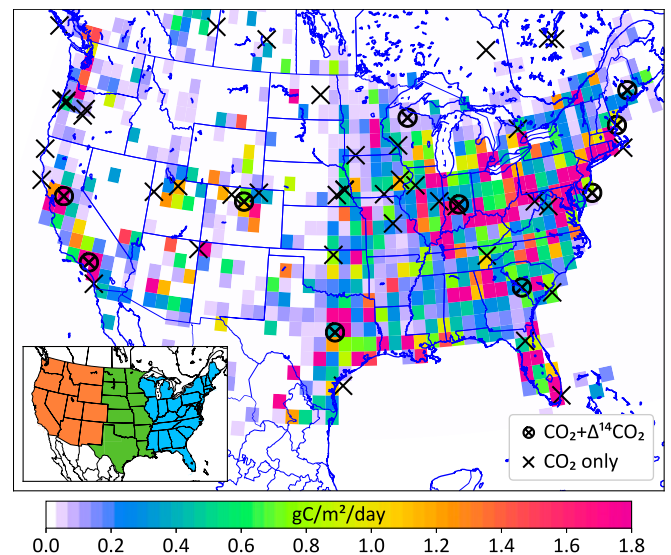


Fig. 1. Mean annual FF CO₂ from the Miller/CT prior of Fig. 2 over and around the United States, along with the location of observing sites with only CO₂ measurements (crosses) and with both CO₂ and Δ¹⁴CO₂ measurements (circled crosses) within the map area in 2010. (*Inset*) The delineation of Western (orange), Central (green), and Eastern (blue) US regions mentioned in the text. The Western US region also contains Hawaii and Alaska.

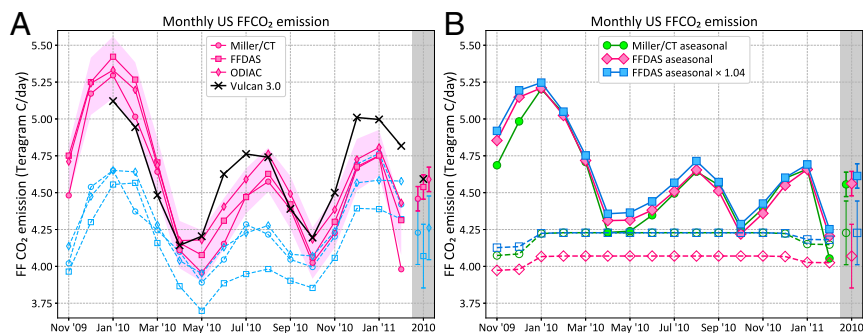


Fig. 2. Monthly prior (dashed lines/open symbols) and optimized (solid lines/filled symbols) US FF CO₂ estimates, along with the 2010 annual totals (gray region to the right). (A) The three pink lines represent the three FF CO₂ estimates starting from three different FF CO₂ priors (blue lines). (B) Results from three alternate aseasonal prior FF CO₂ estimates are shown. The pink shaded region in A denotes $\pm 1\sigma$ analytical uncertainty of optimized monthly FF CO₂, while the error bars in the gray regions denote the same for 2010 annual totals. Values are expressed as daily averages to account for months of varying lengths. Annual aggregate FF CO₂ for the inverse estimates and related priors are given in Table 1. Vulcan 3.0 monthly and annual aggregates are shown in A for comparison to the preferred inverse estimates. Adjustments made to Vulcan FF CO₂ for comparison to atmosphere-derived estimates are described in the text.

Results and Discussion

Fig. 2 presents monthly and annual FF CO₂ estimates (expressed as daily averages) for inversions using Miller/CT, ODIAC, and FFDAS FF CO₂ prior emissions (A), along with results of sensitivity tests using three aseasonal representations of the Miller/CT and FFDAS priors (B). Results from the aseasonal priors show coherent seasonal variation of posterior FF CO₂, indicating that the estimated FF CO₂ seasonality arises from the $\Delta^{14}\text{CO}_2$ observations and not the prescribed prior emissions. We can reject the alternative possibility that the posterior FF CO₂ seasonality is an artifact of seasonal transport bias, since distinct FF CO₂ maxima emerge in both summer and winter when vertical mixing regimes and any associated biases in the modeled transport will differ substantially. Estimated monthly and annual totals are also robust to reasonable bias in the magnitude of the prior emissions, as evidenced by the nearly identical results for two priors with annual FF CO₂ totals that differ by $\sim 4\%$. Furthermore, the experiment in which FFDAS prior emissions have been scaled to match US total emissions of Miller/CT (Fig. 2B) indicates that the posterior estimates are relatively insensitive to inventory-derived differences in the spatial pattern of emissions over the United States (Appendix SI, Fig. S3), despite the limited number and distribution of $\Delta^{14}\text{CO}_2$ observations.

Monthly results for the more realistic, seasonally varying priors (Fig. 2A) are statistically indistinguishable, lying within the 1σ monthly posterior uncertainty of their three-member means for all months, despite differences in the magnitude and timing of prior monthly emissions. The seasonal amplitude of estimated monthly emissions is larger than for results using aseasonal FF CO₂ priors (Fig. 2B) and also larger than the amplitude of all three seasonal FF CO₂ priors. The estimated seasonality is consistent with monthly US aggregates from the updated Vulcan 3.0 emission data product (6), as shown by adjusted Vulcan totals (black symbols in Fig. 2A), which lie at or within 1σ of the atmosphere-derived three-member means for nine of the 12 months of 2010. Notably, both the atmospheric and Vulcan estimates indicate a relative excess of warm season FF CO₂ compared to the prior estimates, suggesting that seasonality imposed on the priors by scaling to CDIAC monthly totals (for FFDAS and ODIAC) or the prescribed seasonal cycle of Miller/CT (21) may both underestimate summertime energy demands. This may be due in part to increases in installed residential air conditioning, which accelerated in most of the country over the last two decades (24). In contrast, while both the inverse results and Vulcan indicate larger cold-season emissions in winter 2009/10 than in winter 2010/11, the disparity is signifi-

cantly greater in the inverse results, as discussed in more detail below.

Table 1 compares annual US FF CO₂ totals for the inverse estimates and from available inventories. The column “FF CO₂ (reported)” gives the US country total FF CO₂ for 2010 as reported by the respective inventories. All “FF CO₂ (reported)” totals except that from Vulcan 3.0 exclude in-country emissions from the combustion of international bunker fuels, in accordance with UNFCCC international reporting guidelines (25). The column “FF CO₂ (adjusted)” reflects an effort to adjust reported values to enable a more direct comparison with the atmosphere-based inverse estimates. As noted earlier, inventories for which gridded products were available (CDIAC, EDGAR 4.2 FT2010, EDGAR 4.3, and Vulcan 3.0) were summed within the same $1^\circ \times 1^\circ$ US country mask used to derive US totals for the inverse estimates. For the two EDGAR inventories, this resulted in a significant increase because, unlike the EDGAR-reported US country totals, the gridded products include emissions from international bunker fuels. For the US EPA inventory, which is not spatially resolved within the United States, we subtracted EPA-reported emissions of 11 TgC yr⁻¹ from US territories (ref. 2, Table 2-10). For CDIAC and the US EPA inventory totals, we added an estimate of in-country emissions from international aviation of 37 TgC yr⁻¹ from the US EPA (18). For Vulcan 3.0, the spatially aggregated total is 1,637 TgC yr⁻¹, which includes 20 TgC yr⁻¹ of emissions from all in-country aviation up to an altitude of 3,000 ft. We estimate the total in-country aviation emission in 2010 to be 79 TgC yr⁻¹ from domestic (42 TgC yr⁻¹ accord-

Table 1. 2010 US FF CO₂ estimates from inversions and inventories

Source	FF CO ₂ , TgC yr ⁻¹			
	Reported	Adjusted	Prior	Posterior
CDIAC	1,471	1,513		
EDGAR 4.2 FT2010	1,497	1,522		
EDGAR 4.3	1,505	1,545		
US EPA	1,555 ⁺⁶² ₋₃₁	1,581 ⁺⁶² ₋₃₁		
Vulcan 3.0	1,638	1,676		
Inverse estimate (mean)			1,528	1,653 \pm 30
Inverse estimate (Miller/CT prior)			1,543	1,627 \pm 30
Inverse estimate (seasonal FFDAS prior)			1,485	1,656 \pm 30
Inverse estimate (ODIAC prior)			1,555	1,675 \pm 30

ing to the US EPA [ref. 2, table 2–13]) and international (37 TgC yr⁻¹, ref. 18) sectors. We therefore added 79 – 20 = 59 TgC yr⁻¹ to Vulcan to account for aviation emissions above 3,000 ft. Furthermore, we subtracted (non-FF CO₂) emissions of 20 TgC yr⁻¹ from combustion of biofuels included in the transportation sector of Vulcan (6). For the inverse estimates, we report aggregated US total FF CO₂ for prior emissions, posterior results, and their three-member means.

The mean atmosphere-derived US FF CO₂ estimate is significantly (> 3σ) greater than adjusted EDGAR and CDIAC totals, but within 1σ of the adjusted Vulcan 3.0 total (Table 1). The atmosphere-derived estimate is also significantly larger than the central US EPA estimate after adjustment, but overlaps its upper 95% confidence limit at 1σ posterior uncertainty. We therefore consider the possibility that the concordance of the inverse estimates and the larger inventories results from an artifact of the inversion setup that might produce a high bias in derived FF CO₂.

Atmospheric transport is a leading source of both random and systematic error in posterior flux estimates (26–28). In this work, we assume that much of the true random transport uncertainty is captured by the model representativeness error, which was derived for each atmospheric measurement as a quantity proportional to the simulated tracer (CO₂ and ¹⁴CO₂) gradient in the vicinity of the measurement location and then propagated into the total posterior uncertainty (*Materials and Methods*). For CO₂, the representativeness error may exceed the measurement uncertainty by a factor of 5 to 15, while for Δ¹⁴CO₂, the two uncertainties are comparable, as a result of greater measurement uncertainty.

Systematic transport errors may lead to biases in estimated fluxes (8, 28, 29), but are difficult to quantify. Here, we provide an assessment of model-transport fidelity by taking advantage of measurements of sulfur hexafluoride (SF₆), a chemically inert molecule, 97% of whose emissions come from the Northern Hemisphere, overwhelmingly from industrialized countries (30). Simulations of the interhemispheric SF₆ gradient using the present version of the Tracer Model 5 (TM5) transport model match the observed latitudinal gradient of 0.30 parts per trillion (ppt) (“TM5 EIC” in figure 2 of ref. 8). Compared to simulated gradients of 0.24 to 0.38 ppt for the range of transport models considered earlier by Patra et al. (31), the current version of TM5 appears to provide a reliable representation of physical processes influencing interhemispheric mixing. More relevant to the current problem of estimating surface fluxes over the continental United States is the ability of the model to represent vertical mixing processes within the domain. In Fig. 3, we show

multiyear average vertical gradients of SF₆ at various US aircraft profiling sites (*SI Appendix, Fig. S2*), computed with respect to the free troposphere (5 to 8 km above sea level). While the model generally recovers the structure of observed vertical gradients, the modeled SF₆ in the lower troposphere tends to be higher than observed. Assuming that these differences arise primarily from model biases in the representation of vertical mixing, this suggests that vertical mixing in the model may be too weak, leading to excess “trapping” of surface emissions within the lower atmosphere. In the context of an inversion, such excessive trapping would lead to an underestimate of the true FF CO₂. Thus, any such vertical transport biases in our system are more likely to lead to posterior FF CO₂ estimates that are biased low rather than high and cannot explain our primary finding of atmosphere-derived US FF CO₂ estimates that are greater than most inventories. Nonetheless, we acknowledge that, despite our effort to represent random transport uncertainty using a formulation for representativeness error, reported posterior flux uncertainties may underestimate the true total FF CO₂ uncertainty due to the challenge of quantifying all possible sources of transport error. We also note that, although the analytical posterior FF CO₂ uncertainties (\hat{B} of Eq. 3 in *Materials and Methods*) for annual and monthly totals of 2 to 4% in Fig. 24 and Tables 1 and 2 are small for an atmospheric inversion, they are consistent with the small prior FF CO₂ uncertainties (5% for the national annual total and 10 to 12% for national monthly totals, as determined from differences between available inventories) and the fact that gradients in atmospheric Δ¹⁴CO₂ over North America are determined almost entirely by recently emitted FF CO₂ (8, 32).

In Table 2, we summarize other potential biases in our system, as represented by the spread (maximum to minimum) between multiple inversions for a wide range of different configurations (*Materials and Methods*). By far the largest of these biases results from an alternate specification of the prior NEE. Use of an alternate NEE prior from the Simple Biosphere-Carnegie-Ames-Stanford Approach (SiB-CASA) biosphere model (33) (as opposed to NEE from the standard CASA model in our default setup, ref. 34) yielded a posterior FF CO₂ estimate that was 86 TgC yr⁻¹ higher than the default estimate when starting from the Miller/CT FF CO₂ prior. The difference between the two NEE priors (–223 TgC yr⁻¹ over the United States in 2010 for SiB-CASA vs. –282 TgC yr⁻¹ for CASA) was well within the range of the specified prior NEE uncertainty (152 TgC yr⁻¹ at 1σ), but the associated FF CO₂ estimates differed by almost three times the estimated FF CO₂ posterior uncertainty. This is most likely because the alternate NEE prior was not merely

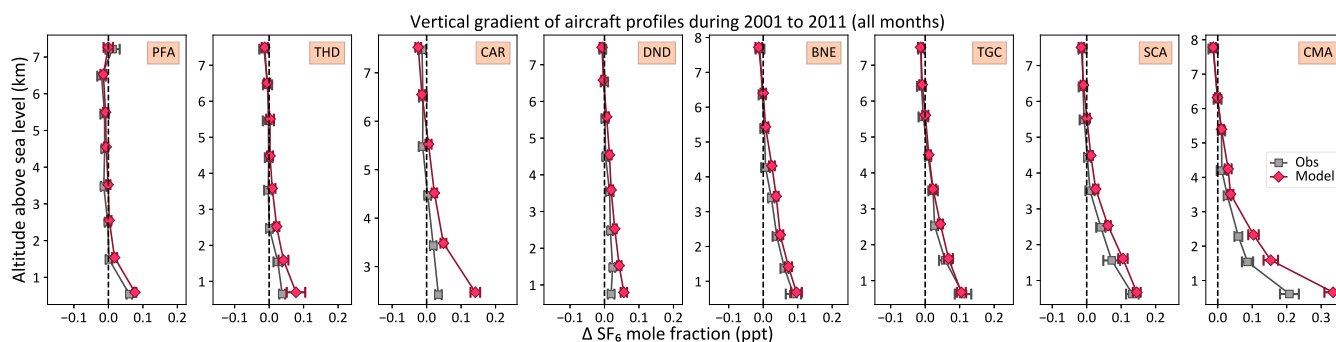


Fig. 3. Modeled and observed (Obs) vertical gradients of SF₆ at eight continental US sites with respect to the mean free troposphere at each site, defined here as observed or simulated mole fractions between 5 and 8 km above sea level. The free tropospheric time series at each site was calculated by fitting a linear trend through the 5- to 8-km SF₆ mole fraction, which was then subtracted from all SF₆ mole fractions between 2001 and 2011 before averaging. The error bars represent twice the standard error in the mean difference between any level and the free troposphere. Site locations and date ranges of the observations are given in *SI Appendix, Fig. S2*. SF₆ emissions used here were from the EDGAR 4.2 inventory (3), after adjusting global totals to match the observed atmospheric growth rate (<https://www.esrl.noaa.gov/gmd/hats/combined/SF6.html>).

Table 2. National and regional FF CO₂ uncertainty and sensitivity to system setup

Region	2010 total FF CO ₂ , TgC yr ⁻¹		Analytical uncertainty				Spread due to prior FF		Spread due to prior NEE				Spread from other sensitivity runs	
			Prior		Posterior				2010 coverage		NRC5000			
	Inversion	Vulcan	TgC yr ⁻¹	%	TgC yr ⁻¹	%	TgC yr ⁻¹	%	TgC yr ⁻¹	%	TgC yr ⁻¹	%	TgC yr ⁻¹	%
United States	1,653	1,676	78.8	5.2	30.2	1.8	56.4	3.4	86.2	5.2	26.3	1.6	29.4	1.8
Eastern US*	889	953	56.2	6.3	26.2	3.0	15.7	1.8	34.3	3.9	18.7	2.1	15.0	1.7
Western US*	302	310	32.8	12.4	12.4	4.1	35.8	11.9	49.9	16.6	7.6	2.5	5.2	1.7
Central US*	463	413	36.1	9.6	19.6	4.2	8.8	1.9	1.9	0.4	0.0	0.0	9.2	2.0

*Eastern, Western, and Central US, as defined in Fig. 1.

a random perturbation of the default prior, and the number of $\Delta^{14}\text{CO}_2$ measurements available in 2010 was not sufficient to detect all systematic differences between the two prior NEE patterns. However, increasing the number of $\Delta^{14}\text{CO}_2$ measurements to $\sim 5,000$ per year in a synthetic data inversion (following Basu et al., ref. 8) reduced the sensitivity of derived FF CO₂ to the specified prior NEE to 22.5 TgC yr⁻¹ (1.4%, as per the “NRC5000” column of Table 2). This suggests that sensitivity to different specifications of the NEE prior is not a limitation of our method, but of $\Delta^{14}\text{CO}_2$ data coverage. Although we cannot rule out a high bias in our 2010 FF CO₂ estimate from differences between our default NEE prior and the (unobserved) true NEE, the alternate prior from SiB-CASA examined here results in the opposite.

Biases in FF CO₂ might also arise from errors in the non-FF fluxes contributing to the measured $\Delta^{14}\text{CO}_2$ (32, 35, 36). However, in our case, all such factors would result in higher FF CO₂ estimates or otherwise negligible adjustments. For example, specification of erroneously large $^{14}\text{CO}_2$ emissions from nuclear power plants may lead to erroneously high FF CO₂ (32, 35, 37). However, total nuclear production of $^{14}\text{CO}_2$ in the United States is more than an order of magnitude smaller than needed to explain the difference between the low-end inventory estimates and the inverse results. An excess of ^{14}C in CO₂ from heterotrophic respiration might also lead to erroneously high FF CO₂, but the analysis of LaFranchi et al. (36) suggests that prior terrestrial isotopic disequilibrium employed here may be biased low rather than high in some regions of North America. This is consistent in sign with a +3.5% adjustment performed on prior US terrestrial disequilibrium fluxes by our inversion system. Neither cosmogenic nor oceanic disequilibrium fluxes produce significant spatial gradients of $\Delta^{14}\text{CO}_2$ over the United States and are therefore highly unlikely to contribute to significant errors in US FF CO₂, as evidenced by sensitivity experiments listed in *Materials and Methods* and summarized in the last column of Table 2. An incorrect initial $^{14}\text{CO}_2$ field could, in principle, impact the first few months of derived FF CO₂. However, sensitivity experiments using a wide range of initial conditions indicate that the tropospheric $\Delta^{14}\text{CO}_2$ distribution in our system adjusts to its observed state in just a few months and well before the start of 2010, suggesting that our FF CO₂ estimates are largely insensitive to the initial condition.

All inverse results in Fig. 2 point to significantly larger monthly emissions in the winter of 2009 to 2010 than in 2010 to 2011, a difference that is more pronounced than in Vulcan and the prior FF CO₂ emissions. For example, the mean difference between US FF CO₂ in January and February 2010 and January and February 2011 from the inverse results is 44 ± 13.7 TgC. In contrast, the difference in aggregated January and February totals from inventories is 7.4 TgC for Vulcan and 14.9 TgC for CDIAC (20). Larger wintertime FF CO₂ in January and February 2010 compared to 2011 could, in principle, be due to lower temperatures

and greater residential and industrial heating and electricity demands. For example, population weighted nationwide heating degree days (HDDs) compiled by the US Energy Information Administration (accessed August 21, 2019) were 1,735 in January and February 2010 compared to 1,694 in January and February 2011. However, the relative difference of +2% in HDDs in January and February of 2010 is unlikely to explain the difference in derived FF CO₂ of $+16 \pm 5\%$, especially since heating-related energy use is only a fraction of total energy use (and therefore FF CO₂). As noted above, the larger-than-expected year-to-year difference in cold-season emissions cannot be attributed to initialization and spin-up of the inverse model and must arise instead from unresolved, transient transport or inventory bias, or some combination of the two.

Distributed atmospheric observations have the potential to resolve emissions at a subnational scale, depending on the number and location of the observations. Table 2 provides mean atmosphere-derived FF CO₂ estimates and associated posterior flux uncertainties for three large subregions of the United States (Fig. 1, *Inset*). Regional posterior flux uncertainties range from 3.0 to 4.2%, which is comparable to estimated uncertainties in national totals from inventories (38) (uncertainties at the subnational scale are rarely specified). Uncertainties for the Eastern US are the smallest (3.0%), a likely result of our early programmatic choice to concentrate observations in and downstream of the region with largest emissions (Fig. 1). Given the observed agreement of the atmosphere-derived estimates and adjusted FF CO₂ totals from Vulcan 3.0 at the national level, Table 2 also includes similarly adjusted regional Vulcan totals for comparison to the inverse results. Since adjustment figures for aviation and non-FF CO₂ from biofuel use (as discussed above) were not available regionally, we approximated regional adjustments by allocating the total national adjustment of +39 TgC yr⁻¹ in proportion to the unadjusted Vulcan regional totals of 931, 403, and 303 TgC yr⁻¹ for the Eastern, Central, and Western US, respectively. The regional comparisons indicate that 1 σ agreement of national totals between the Vulcan and atmosphere-based estimates is due in part to compensatory differences across regions, whereby significantly lower than Vulcan FF CO₂ in the Eastern US is offset by significantly higher than Vulcan values in the Central US (this is also true for unadjusted totals). Although we do not know which result is closer to the true FF CO₂, the finding of compensatory regional differences raises the question of how well the present observing and modeling framework resolves FF CO₂ for different regions. To evaluate this, we considered posterior correlations between regional FF CO₂ estimates derived using the same 110-member inversion ensemble used to derive analytical uncertainties. Large correlations between posterior FF CO₂ estimates would imply that those estimates are not independent, whereas absence of correlation would indicate that they are. As shown by posterior correlations in Table 3, the Western US region is almost entirely decorrelated from the other regions, while negative correlations are larger (approaching -0.3) for

Table 3. Prior and posterior correlation of FF CO₂ between different subregions of the United States, as defined in Fig. 1

Region 1	Region 2	Prior	Posterior
Eastern US	Central US	0.08	-0.27
Eastern US	Western US	0.07	-0.02
Eastern US	Central + Western US	0.10	-0.25
Central US	Eastern US	0.08	-0.27
Central US	Western US	0.04	-0.04
Central US	Eastern + Western US	0.09	-0.26
Western US	Eastern US	0.07	-0.02
Western US	Central US	0.04	-0.04
Western US	Eastern + Central US	0.08	-0.05

the adjacent Central and Eastern US regions. The reduced ability to cleanly separate emissions from the Central and Eastern US regions in the current observing network is likely due to some combination of insufficient observational constraints, the distribution of major FF CO₂ sources, and the mean westerly transport of air over the continent. FF CO₂ is independently resolved for the Western US, but displays large sensitivity to the choice of prior NEE (Table 2), likely because 2010 $\Delta^{14}\text{CO}_2$ coverage in the Western US was relatively sparse. However, expansion to “NRC5000” coverage (8) appears to reduce that sensitivity dramatically. FF CO₂ regional flux uncertainty and regional resolution of fluxes can be improved in all regions given additional measurement coverage, as demonstrated by earlier OSSE results that consider the accuracy of derived fluxes (8).

In addition to providing independent estimates of FF CO₂, the dual-tracer system is expected to reduce potential biases in estimated NEE that would otherwise arise from differences between specified (fixed) FF CO₂ and true FF CO₂ in a CO₂-only inversion (8, 39, 40). Lacking independent constraints on the true NEE, we cannot claim that posterior NEE for 2010 from our dual-tracer inversion is more accurate than from other CO₂-only inversion frameworks. However, we can estimate the size of a potential NEE bias that might arise in a more traditional single-tracer framework by performing a CO₂-only inversion with our system, with FF CO₂ fixed to its prescribed prior values and without assimilating $\Delta^{14}\text{CO}_2$ data. Fig. 4 compares the total CO₂ flux and NEE in 2010 from the dual-tracer and CO₂-only inver-

sions, using Miller/CT FF CO₂ prior emissions in both cases. While the national total CO₂ flux changes little with the introduction of $\Delta^{14}\text{CO}_2$ data, derived NEE changes by 75 TgC yr⁻¹. This is larger than the 59 TgC yr⁻¹ adjustment from the prior to the posterior NEE in the CO₂-only inversion and more than twice the posterior NEE uncertainty of 32 TgC yr⁻¹. This suggests that the size of the NEE error made in a CO₂-only inversion by prescribing FF CO₂ can be significant compared to estimated NEE, its uncertainty, and its interannual variation. For example, the 1 σ variation of temperate North American NEE between 2000 and 2016 according to NOAA’s CarbonTracker 2017 (accessed April 30, 2019) is 200 TgC yr⁻¹, while the mean sink is 320 TgC yr⁻¹.

Conclusions

We have determined US national emissions of FF CO₂ based on measurements of atmospheric CO₂ and $\Delta^{14}\text{CO}_2$ and a dual-tracer inversion framework that solves for both FF CO₂ and NEE simultaneously (8). Our atmosphere-derived estimate of US national total FF CO₂ emissions in 2010 of 1,653 \pm 30 TgC yr⁻¹ is significantly ($> 3\sigma$) larger than from EDGAR 4.2 FT2010, EDGAR 4.3.2, and CDIAC, even after adjustments that attempt to account for missing emissions in the inventories. Our derived US FF CO₂ total is also larger than a similarly adjusted central estimate from the US EPA, but overlaps its reported upper 95% confidence limit. In contrast, our result is consistent at 1 σ with a similarly adjusted US annual total FF CO₂ aggregated from the latest release of the Vulcan 3.0 data product, with monthly totals that are within 1 σ for nine of the 12 months. Of all of the tested sources of bias in our observing and assimilation system, the choice of prior NEE has the largest impact on estimated FF CO₂. Although we cannot rule out a high bias in our FF CO₂ estimate arising from differences between our default choice of prior NEE and the (unobserved) true NEE for 2010, use of an alternative prior NEE resulted in higher, rather than lower, FF CO₂. We also demonstrate that the impact of prior NEE on derived FF CO₂ is not an inherent limitation of our assimilation system but, rather, of present $\Delta^{14}\text{CO}_2$ data coverage. Increasing the number of North American $\Delta^{14}\text{CO}_2$ observations from \sim 1,000 to \sim 5,000, as recommended by the US National Academy of Sciences (17), reduces FF CO₂ sensitivity to prior NEE to levels consistent with estimated random posterior FF CO₂ uncertainties of less than 2%.

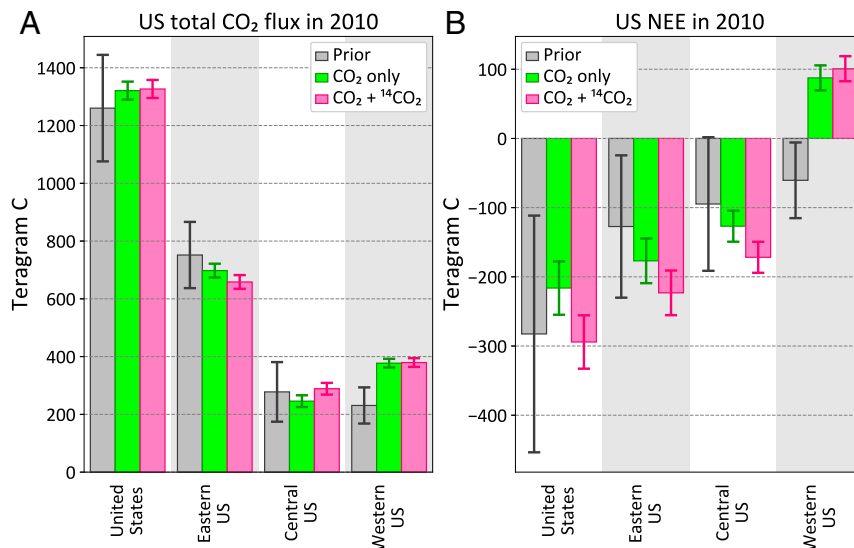


Fig. 4. The annual total CO₂ flux (A) and the NEE (B) from two inversions, for the United States and the three large subdivisions of Fig. 1. The “CO₂+¹⁴CO₂” inversion is the dual tracer Miller/CT inversion of Fig. 2A, while the “CO₂ only” inversion is the same inversion without $\Delta^{14}\text{CO}_2$ data and FF CO₂ optimization.

Agreement between the atmosphere-derived US FF CO₂ emissions estimate for 2010 and that from Vulcan 3.0 is encouraging, but by no means definitive. A fuller evaluation will require comparison over several years. This should also include an effort to reconcile atmosphere- and Vulcan-derived results with those from the US EPA, which is tasked with providing US emissions of CO₂ and several other GHGs annually as part of our international reporting obligation to the UNFCCC. By far, the largest component of the total CO₂-equivalent emissions for all US EPA-reported gases is FF CO₂, for which the US EPA indicates a decline of ~10% per decade since 2007. Estimated uncertainties for individual annual FF CO₂ totals are -2% to +5% at the 95% confidence limit (ref. 2, table A-284), suggesting that US EPA-reported trends outside that range should be robust (assuming that any systematic accounting biases do not change over time). Verification of annual totals and multiyear trends using independent methods would promote confidence in the objectivity and transparency of emissions reporting and help to guide present and future emissions-mitigation measures and related policy. Furthermore, while the US EPA provides important sectoral information on emissions, and inventories are updated annually within ~16 months of the year of record, they report annual, national totals only. An expanded $\Delta^{14}\text{CO}_2$ measurement network and data assimilation effort would permit timely FF CO₂ estimation at the scale of several contiguous US states (8), providing independent and objective guidance to entities such as the state of California (7) and the Regional Greenhouse Gas Initiative. Any expanded effort must also include a fuller examination of transport-related uncertainties, including the implementation and assessment of additional atmospheric transport models. In the case of the model transport used here, we have demonstrated, based on comparisons to SF₆, that both interhemispheric exchange rates and vertical transport over the continent are well represented by the model, and any remaining systematic biases would likely lead to underestimation rather than overestimation of FF CO₂ in our system. While systematic transport errors may influence absolute emissions estimates, detection of interannual emissions trends is expected to be more robust (41), satisfying a principal requirement of emissions-reduction verification and assessment of mitigation policies.

Materials and Methods

We used a variational dual-tracer CO₂ and ¹⁴CO₂ inversion system based on the TM5 atmospheric transport model to estimate FF CO₂ fluxes (8). The system estimates the optimal flux \bar{x}_{opt} by minimizing a "cost function" J

$$J = \frac{1}{2} (H\bar{x} - \bar{y})^T R^{-1} (H\bar{x} - \bar{y}) + \frac{1}{2} (\bar{x} - \bar{x}_0)^T B^{-1} (\bar{x} - \bar{x}_0) \quad [1]$$

as a function of fluxes \bar{x} , given a prior flux \bar{x}_0 , observations \bar{y} , atmospheric transport and observation operator H , covariance of prior flux errors B , and covariance of observation errors R , where R includes representativeness errors in H (42). The optimal state \bar{x}_{opt} and its posterior covariance \hat{B} are given by

$$\bar{x}_{\text{opt}} = \bar{x}_0 + BH^T (R + HBH^T)^{-1} (\bar{y} - H\bar{x}_0) \quad [2]$$

$$\hat{B} = (B^{-1} + H^T R^{-1} H)^{-1}. \quad [3]$$

For our problem, \bar{y} included observations of CO₂ and CO₂ · $\Delta^{14}\text{CO}_2$ (8), and H was the TM5 transport model ("TM5 EIC" of ref. 8) driven by European Centre for Medium-Range Weather Forecasts ERA-Interim meteorology. Prior fluxes for CO₂ and ¹⁴CO₂ (\bar{x}_0) were as described in ref. 8, but with prior NEE and oceanic CO₂ fluxes updated to those of CarbonTracker 2016. Of the three FF CO₂ priors used to construct our reported estimates (Fig. 2A), the mean annual FF CO₂ for the US portion of Miller/CT is shown in Fig. 1, and differences between the other two priors (ODIAC and FFDAS) and Miller/CT are shown in *SI Appendix, Fig. S3*. While the difference in the annual US total between the three inventories is less than 5% (Table 1), regional differences can be significantly larger (Table 2) and

grid scale differences larger still (*SI Appendix, Fig. S1*). Prior FF CO₂ uncertainties were determined from the spread across available inventories for each grid cell (similar to the subset of three inventories in *SI Appendix, Fig. S1*), and spatiotemporal correlations were assigned between the grid cells such that the 1 σ prior uncertainty on the 2010 US annual total was 5%. The uncertainties of all of the other fluxes (B) are as in ref. 8. Prior isotopic fluxes include those for land and ocean disequilibria, and nuclear and cosmogenic ¹⁴CO₂ production, but only the disequilibrium fluxes were optimized. The inversion was run from July 1, 2009 to April 1, 2011 to estimate fluxes in 2010 with a spin-up (-down) period of 6 (3) months. The initial fields of CO₂ and ¹⁴CO₂ on July 1, 2009, were taken from the posterior mole fraction fields of another CO₂+ $\Delta^{14}\text{CO}_2$ inversion for the period January 1, 2008 to July 1, 2009. TM5 was run at 3° × 2° globally and 1° × 1° over North America. A total of 167,573 CO₂ and 1,504 $\Delta^{14}\text{CO}_2$ observations were assimilated after screening for model-representation issues, as described below. CO₂ observations are from NOAA's ObsPack GV+3.2 (43), spanning 180 different sites managed by 31 different principal investigators across multiple agencies and laboratories. Sampling platforms and associated sampling frequencies are summarized in *SI Appendix, Table S1*. At most sites, only midafternoon CO₂ observations were assimilated since they represent well-mixed planetary boundary layers and a large surface footprint. However, at mountaintop sites, only late night and early morning CO₂ observations were assimilated in order to avoid signals associated with upslope winds. $\Delta^{14}\text{CO}_2$ observations came from 16 different sites, measured by three different laboratories, as summarized in *SI Appendix, Table S2*. The observations assimilated are provided in *Dataset S1*. At MWO (1,728 m above sea level), only nighttime samples were included in order to avoid large urban signals from Los Angeles during the day. Similarly, other $\Delta^{14}\text{CO}_2$ samples influenced by local urban signals were identified and removed from the analysis by using comeasured CO as a proxy for pollution, as illustrated for Niwot Ridge, Colorado (NWR) in *SI Appendix, Fig. S4*. All $\Delta^{14}\text{CO}_2$ measurements were assigned an uncertainty of 1.8‰ (15), except for the Cape Grim background site in Australia (CGO) and Barrow, Alaska, for which individual reported measurement uncertainties (typically larger than 1.8‰) were used. For both tracers, a random transport-model error computed from modeled tracer gradients across neighboring cells was added in quadrature to the measurement uncertainties to construct R in Eq. 1. We evaluated the precision of our emission estimates by running an ensemble of 110 inversions, in which we randomly perturbed prior fluxes (\bar{x}_0) and measurements (\bar{y}). Perturbed prior fluxes were generated as $\bar{x}_{0,\text{perturb}} = L\bar{\xi} + \bar{x}_0$, where $B = LL^T$ and $\bar{\xi}$ is a standard normal random vector. Measurement perturbations consistent with R were applied to \bar{y} . Perturbations of individual tracers were assumed uncorrelated in time. However, since R includes representativeness errors, perturbations of CO₂ and CO₂ · $\Delta^{14}\text{CO}_2$ are correlated in cases where CO₂ variations are primarily driven by transported FF CO₂. We evaluated these correlations in two steps: 1) We simulated CO₂ and ¹⁴CO₂ for 3 years (July 1, 2009 to July 1, 2012) with prior fluxes to generate continuous time series of CO₂ and CO₂ · $\Delta^{14}\text{CO}_2$ at each site. 2) We then subtracted a LOWESS (locally weighted scatterplot smoothing) smoothed curve from the time series and evaluated the correlation between the residuals for each season and site. *SI Appendix, Fig. S5* shows the scatter plot and correlation between the residuals at NWR. As expected, the cross-tracer correlation is near zero in the summer when CO₂ variations are overwhelmingly driven by the biosphere and close to -1 in the winter when FF CO₂ and ecosystem respiration contribute roughly equally to CO₂ enhancements (32). These site- and season-specific correlations were used to populate off-diagonal elements of R connecting CO₂ and CO₂ · $\Delta^{14}\text{CO}_2$ measurements from the same air sample. Since the posterior uncertainty in fluxes depends only on H , B , and R , the uncertainty of all inversion results assimilating the same observations and using the same transport will be the same. We therefore derived the analytical uncertainty using the Miller/CT FF CO₂ prior only, as the standard deviation of posterior FF CO₂ across the 110 ensemble members (Table 2). The sensitivity of estimated FF CO₂ to the choice of FF CO₂ and NEE priors was presented in Table 2. The column "Spread from all other sensitivity runs" includes possible errors in FF CO₂ estimates stemming from other choices made in the inverse setup, including the vertical profile of cosmogenic ¹⁴CO₂ production, the initial CO₂ and ¹⁴CO₂ fields, and an alternate specification of ¹⁴CO₂ disequilibrium-flux uncertainty. Our default cosmogenic ¹⁴CO₂ production profile distributed the production equally between the stratosphere and the troposphere. In addition, we performed an inversion where the production was confined to the stratosphere alone. Default initial CO₂ and $\Delta^{14}\text{CO}_2$ fields on July 1, 2009, came from the end of an 18-month dual-tracer inversion, as described above. In addition, we ran an inversion with initial fields from a decadal forward run with time-varying prior fluxes starting on January 1, 2000. Finally,

we ran our inversion with looser and tighter error specifications on the prior ocean disequilibrium flux. The full ensemble spread (maximum to minimum) of posterior FF CO₂ across these experiments was small, as expected, since the alternate treatments have little impact on $\Delta^{14}\text{CO}_2$ gradients over North America.

Data Availability. CO₂ data used here are from NOAA's CO₂ ObsPack GV+3.2 2017-11-02, after filtering and data selection, as detailed in *Materials and Methods*. $\Delta^{14}\text{CO}_2$ measurements assimilated in the inversions are included in *SI Appendix*. The TM5 4DVAR source-sink inversion framework used here is open source and publicly accessible (<https://sourceforge.net/projects/tm5/>).

1. United Nations Framework Convention on Climate Change, Report of the Conference of the Parties on its nineteenth session, held in Warsaw from 11 to 23 November 2013. Addendum. Part two: Action taken by the Conference of the Parties at its nineteenth session. (United Nations, Warsaw, Poland, 2013).
2. Environmental Protection Agency, "Inventory of US greenhouse gas emissions and sinks" (EPA Tech. Rep., Environmental Protection Agency, Washington, DC, 2018).
3. M. Muntean et al., "Fossil CO₂ emissions of all world countries—2018 report" (JRC Science for Policy Report, European Commission, Ispra, Italy, 2018).
4. T. Boden, R. Andres, "Global, regional, and national fossil-fuel CO₂ emissions" (Tech. Rep., Carbon Dioxide Information Analysis Center, Oak Ridge National Laboratory, U.S. Department of Energy, Oak Ridge, TN, 2017).
5. K. R. Gurney et al., High resolution fossil fuel combustion CO₂ emission fluxes for the United States. *Environ. Sci. Technol.* **43**, 5535–5541 (2009).
6. K. R. Gurney et al., Replication Data for: Estimating US Fossil Fuel CO₂ Emissions from Measurements of ¹⁴C in Atmospheric CO₂. Harvard Dataverse, V1 (2020). <https://doi.org/10.7910/DV/NEDAP3>. Accessed 19 May 2020.
7. H. Graven et al., Assessing fossil fuel CO₂ emissions in California using atmospheric observations and models. *Environ. Res. Lett.* **13**, 65007 (2018).
8. S. Basu, J. B. Miller, S. Lehman, Separation of biospheric and fossil fuel fluxes of CO₂ by atmospheric inversion of CO₂ and $\Delta^{14}\text{CO}_2$ measurements: Observation system simulations. *Atmos. Chem. Phys.* **16**, 5665–5683 (2016).
9. P. P. Tans, I. Y. Fung, T. Takahashi, Observational constraints on the global atmospheric CO₂ budget. *Science* **247**, 1431–1438 (1990).
10. W. Peters et al., An atmospheric perspective on North American carbon dioxide exchange: CarbonTracker. *Proc. Natl. Acad. Sci. U.S.A.* **104**, 18925–18930 (2007).
11. P. Peylin et al., Global atmospheric carbon budget: Results from an ensemble of atmospheric CO₂ inversions. *Biogeosciences* **10**, 6699–6720 (2013).
12. I. Levin, B. Kromer, M. Schmidt, H. Sartorius, A novel approach for independent budgeting of fossil fuel CO₂ over Europe by ¹⁴CO₂ observations. *Geophys. Res. Lett.* **30**, 2194 (2003).
13. J. C. Turnbull et al., Comparison of ¹⁴CO₂, CO, and SF₆ as tracers for recently added fossil fuel CO₂ in the atmosphere and implications for biological CO₂ exchange. *Geophys. Res. Lett.* **33**, L01817 (2006).
14. H. D. Graven et al., Vertical profiles of biospheric and fossil fuel-derived CO₂ and fossil fuel CO₂:CO ratios from airborne measurements of $\Delta^{14}\text{C}$, CO₂ and CO above Colorado, USA. *Tellus B* **61**, 536–546 (2009).
15. S. J. Lehman et al., Allocation of terrestrial carbon sources using ¹⁴CO₂: Methods, measurement, and modeling. *Radiocarbon* **55**, 1484–1495 (2013).
16. J. C. Turnbull et al., A new high precision ¹⁴CO₂ time series for North American continental air. *J. Geophys. Res. Atmos.* **112**, (2007).
17. Committee on Methods for Estimating Greenhouse Gas Emissions, *Verifying Greenhouse Gas Emissions: Methods to Support International Climate Agreements* (National Academies Press, Washington, DC, 2010).
18. T. Oda, S. Maksyutov, R. J. Andres, The open-source data inventory for anthropogenic CO₂, version 2016 (ODIAC2016): A global monthly fossil fuel CO₂ gridded emissions data product for tracer transport simulations and surface flux inversions. *Earth Syst. Sci. Data* **10**, 87–107 (2018).
19. S. Asefi-Najafabady et al., A multiyear, global gridded fossil fuel CO₂ emission data product: Evaluation and analysis of results. *J. Geophys. Res. Atmos.* **119**, 10,213–10,231 (2014).
20. R. Andres, T. Boden, "Monthly fossil-fuel CO₂ emissions: Mass of emissions gridded by one degree latitude by one degree longitude" (Tech. Rep., Carbon Dioxide Information Analysis Center, Oak Ridge National Laboratory, US Department of Energy, Oak Ridge, TN, 2016).
21. T. J. Blasing, C. T. Broniak, G. Marland, "Estimates of monthly CO₂ emissions and associated $\delta^{13}\text{C}$ values from fossil-fuel consumption in the U.S.A." in *Trends: A Compendium of Data on Global Change* (Carbon Dioxide Information Analysis Center, Oak Ridge National Laboratory, U.S. Department of Energy, Oak Ridge, TN, 2005).
22. M. Krol et al., The two-way nested global chemistry-transport zoom model TM5: algorithm and applications. *Atmos. Chem. Phys.* **5**, 417–432 (2005).
23. Energy Information Administration, "Monthly energy review (September 2019)" (Tech. Rep., Energy Information Administration, Washington, DC, 2019).
24. Energy Information Administration, "Air conditioning in nearly 100 million U.S. homes" (Tech. Rep., Energy Information Agency, Washington, DC, 2011).
25. United Nations Framework Convention on Climate Change, "UNFCCC reporting guidelines on annual inventories for parties included in annex I to the Convention" (Tech. Rep., United Nations Framework Convention on Climate Change, Bonn, Germany, 2013).
26. P. Peylin, D. Baker, J. Sarmiento, P. Ciais, P. Bousquet, Influence of transport uncertainty on annual mean and seasonal inversions of atmospheric CO₂ data. *J. Geophys. Res.* **107**, 4385 (2002).
27. S. Basu et al., The impact of transport model differences on CO₂ surface flux estimates from OCO-2 retrievals of column average CO₂. *Atmos. Chem. Phys.* **18**, 7189–7215 (2018).
28. A. E. Schuh et al., Quantifying the impact of atmospheric transport uncertainty on CO₂ surface flux estimates. *Global Biogeochem. Cycles* **33**, 484–500 (2019).
29. T. Lauvaux, K. J. Davis, Planetary boundary layer errors in mesoscale inversions of column-integrated CO₂ measurements. *J. Geophys. Res.: Atmosphere* **119**, 490–508 (2014).
30. J. G. Olivier, G. Janssens-Maenhout, CO₂ "Emissions from fuel combustion—2012 edition" (IEA CO₂ Report 2012, Part III, Greenhouse-Gas Emissions, International Energy Agency, Paris, France, 2012).
31. P. K. Patra et al., TransCom model simulations of CH₄ and related species: linking transport, surface flux and chemical loss with CH₄ variability in the troposphere and lower stratosphere. *Atmos. Chem. Phys.* **11**, 12813–12837 (2011).
32. J. B. Miller et al., Linking emissions of fossil fuel CO₂ and other anthropogenic trace gases using atmospheric ¹⁴CO₂. *J. Geophys. Res.* **117**, D08302 (2012).
33. I. R. van der Velde et al., Terrestrial cycling of ¹³CO₂ by photosynthesis, respiration, and biomass burning in SiBCASA. *Biogeosciences* **11**, 6553–6571 (2014).
34. K. Schaefer et al., Combined Simple Biosphere/Carnegie-Ames-Stanford Approach terrestrial carbon cycle model. *J. Geophys. Res. Biogeosciences* **113**, G03034 (2008).
35. H. D. Graven, N. Gruber, Continental-scale enrichment of atmospheric ¹⁴CO₂ from the nuclear power industry: Potential impact on the estimation of fossil fuel-derived CO₂. *Atmos. Chem. Phys.* **11**, 12339–12349 (2011).
36. B. W. LaFranchi et al., Strong regional atmospheric ¹⁴C signature of respired CO₂ observed from a tall tower over the midwestern United States. *J. Geophys. Res.: Biogeosci.* **121**, 2275–2295 (2016).
37. F. R. Vogel, I. Levin, D. E. J. Worthy, Implications for deriving regional fossil fuel CO₂ estimates from atmospheric observations in a hot spot of nuclear power plant ¹⁴CO₂ emissions. *Radiocarbon* **55**, 15561572 (2013).
38. R. J. Andres, T. A. Boden, D. Higdon, A new evaluation of the uncertainty associated with CDIAC estimates of fossil fuel carbon dioxide emission. *Tellus B* **66**, 23616 (2014).
39. R. L. Thompson et al., Topdown assessment of the Asian carbon budget since the mid 1990s. *Nat. Commun.* **7**, 10724 (2016).
40. T. Saeki, P. K. Patra, Implications of overestimated anthropogenic CO₂ emissions on east Asian and global land CO₂ flux inversion. *Geosci. Lett.* **4**, 9 (2017).
41. D. F. Baker et al., TransCom 3 inversion intercomparison: Impact of transport model errors on the interannual variability of regional CO₂ fluxes, 1988–2003. *Global Biogeochem. Cycles* **20**, GB1002 (2006).
42. J. F. Meirink, P. Bergamaschi, M. C. Krol, Four-dimensional variational data assimilation for inverse modelling of atmospheric methane emissions: Method and comparison with synthesis inversion. *Atmos. Chem. Phys.* **8**, 6341–6353 (2008).
43. NOAA Earth System Research Laboratory, Global Monitoring Division, Cooperative Global Atmospheric Data Integration Project (2017): Multi-laboratory compilation of atmospheric carbon dioxide data for the period 1957–2016; ObsPack CO₂ GV+ v3.2 2017-11-02 (National Oceanographic and Atmospheric Administration, Washington, DC, 2017).